Synthesis, Characterization, and Comparative Study of Conducting Polyaniline/Lead Titanate and Polyaniline–Dodecylbenzenesulfonic Acid/Lead Titanate Composites

C. Basavaraja, R. Pierson, Do Sung Huh

Department of Chemistry and Institute of Functional Materials, Inje University, Kimhae 621749, Kyungnam, South Korea

Received 26 December 2006; accepted 12 October 2007
DOI 10.1002/app.27582
Published online 22 January 2008 in Wiley InterScience (www.interscience.wiley.com).

ABSTRACT: To study the effect of a surfactant on the properties of polyaniline (PANI)/metal oxide composites, PANI/lead titanate ($PbTiO_3$) composites were synthesized with different weight percentages (10, 20, 30, 40, and 50 wt %) of $PbTiO_3$ in both the absence and presence of dodecylbenzenesulfonic acid (DBSA) by the polymerization of aniline with ammonium persulfate as an initiator. The structural characteristics and stability, surface characteristics, and electric properties of PANI/$PbTiO_3$ and PANI–DBSA/$PbTiO_3$ were studied and compared. The interfacial interactions and thermal stability of these composites were characterized with X-ray diffraction, scanning electron microscopy, transmission electron microscopy, and thermogravimetry techniques. The results indicate significant changes in the physicochemical properties of the composites with the incorporation of DBSA. © 2008 Wiley Periodicals, Inc. J Appl Polym Sci 108: 1070–1078, 2008

Key words: composites; conducting polymers; dielectric properties; mechanical properties; surfactants; thermogravimetric analysis (TGA)

INTRODUCTION

Intrinsically conducting polymers[1,2] such as polyaniline (PANI) and polypyrrole, known as synthetic metals, have been the subject of extensive theoretical and experimental studies in recent years. The physical properties of conducting polymers have been improved significantly through blending with one or more insulating materials,[3] and the results are called polymer composites.[3] Since the discovery of metallic conductivity by the addition of suitable dopants,[4] polymer composites have become promising materials for microelectronic devices such as light-emitting diodes,[5,6] thin-film transistors,[7] gas sensors,[8] and organic transparent electrodes.[9,10] However, the process for synthesizing composite materials is not so easy. Moreover, they have lower solubility in an aqueous solution in comparison with other polymer materials. The dispersion of intrinsically conducting polymers in thermoplastic polymers to form blends has been proved to be one of the most useful procedures for overcoming the solubility problem, and the blends can have several technical applications in the protection of metal corrosion, printed-board circuits, and so forth.[11,12]

However, these blends exhibit lower electric properties in comparison with inorganic conducting materials or coating materials. In this approach, functionalized protonic acids, which can usually serve as surfactants, have also been used instead of inorganic acids[13] for doping in the polymer network of PANI. Camphorsulfonic acid,[14] dodecylbenzenesulfonic acid (DBSA),[15,16] and other acids with long alkyl chains are used for this purpose. The PANI–DBSA complex can be achieved by mechanical mixing or solution mixing on the emeraldine base of PANI with DBSA[16] or through a thermal doping process.[17] It has been shown that long aliphatic chains of DBSA facilitate the process for the PANI–DBSA complex in a conventional way,[18] and the long hydrocarbon tail of DBSA easily modifies the polymer–polymer interface in the complex.[19]

The metal–PANI systems are attracting growing interest because of their advanced mechanical and chemical properties for more potential applications.[20,21] A common feature for many applications is induced by direct contact between PANI and metal oxide films. Thus, understanding the metal–PANI interfacial structure is a very significant subject for various scientific and technological interests. Various techniques have been adopted to obtain better processability and better electrical properties of the metal–PANI composites.[22–24] In addition, Fusalba and Bėlanger[24] reported that a surfactant such as DBSA can also modify the PANI–metal interactions because the metal oxide particles can coalesce with the surfactant during the polymerization process. Surfactant molecules can assemble themselves as an

Correspondence to: D. S. Huh (chemhds@inje.ac.kr).

Journal of Applied Polymer Science, Vol. 108, 1070–1078 (2008)
© 2008 Wiley Periodicals, Inc.

ordered structure with particular morphologies in a solution because of their hydrophilic and lipophilic properties.

Recently, surfactants have also been employed as soft templates for self-assemblies to control the size and shape of nanoparticles. This is called the wet chemical method.[25] The surfactant may control the polymerization condition, kinetics, and final properties of the conjugated polymers. On the basis of the results, the potential incorporation of a surfactant into a conducting polymer improves the electrical, thermooxidative, and hydrolytic stability of the composite because of the introduction of a bulky hydrophobic component.[25–27]

Among many metal oxide materials, lead titanate ($PbTiO_3$), being a ferroelectric material with a perovskite structure, has received a great deal of attention because of its unique combination of piezoelectric, pyroelectric, dielectric, and electro- and acousto-optic properties.[28,29] $PbTiO_3$ is a very attractive material that could be used in a wide variety of applications, including ultrasonic sensors, infrared detectors, electro-optic modulators, and ferroelectric random access memory.[30]

To study the effect of DBSA on the structure and thermal and electrical properties of conducting polymer composites, composites of PANI with $PbTiO_3$ (PANI/$PbTiO_3$) were synthesized in both the absence and presence of DBSA (PANI–DBSA/$PbTiO_3$). The composites were synthesized with different weight percentages (10, 20, 30, 40, and 50 wt %) of $PbTiO_3$ by the addition of a fine-grade powder of $PbTiO_3$ to the polymerization reaction. The obtained composites were characterized with X-ray diffraction (XRD), scanning electron microscopy (SEM), and transmission electron microscopy (TEM). The alternating-current conducting properties of the composites were studied at room temperature at different frequencies. The thermal stability and degradation behaviors of the composites were studied with thermogravimetric analysis (TGA). The thermal degradation process of the composites proceeded in three steps. In addition, the composites were more thermally stable than pure PANI or PANI–DBSA. However, the conducting properties were increased by the addition of DBSA in the composites through the formation of the PANI–DBSA complex.

EXPERIMENTAL

Synthesis of PANI/$PbTiO_3$ and PANI–DBSA/$PbTiO_3$ composites

Aniline, DBSA, $PbTiO_3$, and ammonium persulfate (APS) were purchased from Sigma–Aldrich (USA) and used without further purification. Undoped PANI was obtained by the polymerization of aniline in an aqueous medium[16] with 0.05*M* aniline. Before the process of varying the weight percentage of $PbTiO_3$ in the composites, the dry yield of PANI was confirmed. For the synthesis of PANI/$PbTiO_3$ composites, aniline was placed in a beaker containing water and a fine powder of $PbTiO_3$ (10, 20, 30, 40, or 50 wt %), which was added slowly with constant stirring to obtain a uniform dispersion. Afterwards, the initiator APS (2.5*M*) was added dropwise to process the polymerization of aniline.[16] In the case of the PANI–DBSA/$PbTiO_3$ composites, 0.025*M* DBSA (which was fixed in this experiment) was placed together with the aniline solution and stirred to obtain a uniform dispersion of aniline–DBSA.[31] Later, the APS was added in a similar fashion after the addition of the $PbTiO_3$ powder. The polymerization process was carried out for about 8 h at $\sim 0^{\circ}C$. A precipitated polymer powder was recovered by vacuum filtration and washed thoroughly with deionized water and acetone. Finally, the resulting powder was dried in a vacuum oven for 24 h to achieve a constant weight.

Because the use of HCl media in the polymerization process may cause a doping effect of the chloride ions in the composites, the composites and pure PANI were synthesized in an aqueous medium,[32,33] and the percentage of doped aniline was taken as a constant throughout the synthesis. The molar ratio of aniline (monomer) to DBSA (surfactant) was kept at 2.0 throughout the process for the preparation of the composites. Figure 1 shows a schematic model for the structure of the PANI–DBSA/$PbTiO_3$ composite. It indicates that the micellar structure of DBSA stabilizes the dispersion of PANI and $PbTiO_3$ by incorporating PANI and by encapsulating PANI/$PbTiO_3$ in the matrix, as indicated in the figure.

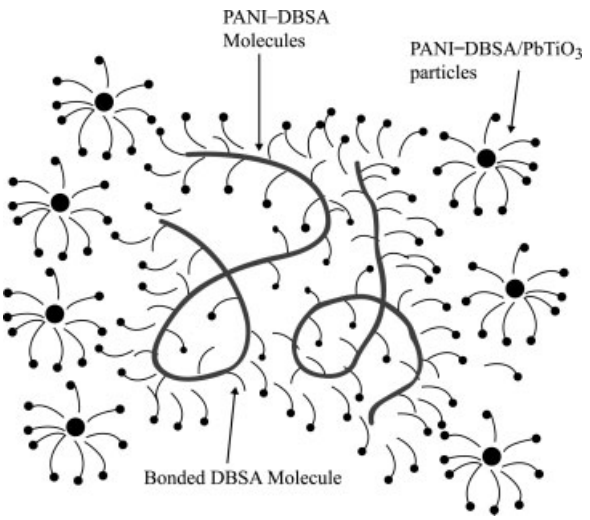

Figure 1 Schematic model for the PANI–DBSA/$PbTiO_3$ composite structure.

Methods used to characterize and measure the electric properties of the composites

The obtained composites were characterized with XRD patterns by a Philips (Netherlands) X-ray diffractometer using Cu Kα radiation (λ = 1.5406 Å). The diffractogram was recorded in terms of 2θ in the range of 10–80° with a scanning rate of 2°/min. The powder morphology of the synthesized composites was investigated with SEM (XL-30 ESEM, Philips) and TEM (JEM-2010, JEOL, Japan). The thermal behavior of the composites was studied with TGA (model 2050, TA Instruments, USA) at a heating rate of 10°C/min.

Powder samples of pure PANI and PANI/$PbTiO_3$ composites were crushed and finely ground in an agate mortar. They were pressed to form pellets 10 mm in diameter and 1–2 mm thick by the application of a pressure of 9 MPa in a hydraulic press. Thereafter, the pellets were coated with silver paste on both sides, and copper electrodes were placed on either surface to obtain better contact. The electrical resistivity was measured with an impedance analyzer (4191A, Hewlett–Packard) in the frequency range of 10^2–10^6 Hz at room temperature.

RESULTS AND DISCUSSION

Characterization and comparison of the composite materials

Figure 2 shows XRD patterns for pure PANI, PANI/$PbTiO_3$ (50%), PANI–DBSA, and PANI–DBSA/$PbTiO_3$ (50%) and expanded portions for PANI/$PbTiO_3$ (50%) and PANI–DBSA/$PbTiO_3$ (50%), which show the increased crystallinity after the incorporation of DBSA into the polymerization process. The diffraction pattern for PANI has a broad peak at about 25 and 19 (2θ values). This may be due to the residual ordered DBSA after doping.[33] The prominent peaks correspond to 2θ = 32.72 with a *d*-spacing value of 2.84 Å. This is due to (110), the plane of the perovskite structure, and the peak at 2θ = 56.48 with a *d*-spacing of 1.637 Å corresponds to (222), the plane of the pyrochlore structure of $PbTiO_3$.[34] These results confirm that the nature of polycrystalline oxide is also observed in these composites similarly to the cases of PANI–V_2O_5[35] and PANI–MoO_3.[36] The increased crystallinity in the case of composites is basically due to the incorporation of $PbTiO_3$ into the polymer matrix, and this is supported by the previous results.[22,23,34–36] However, the effect is more emphasized in this study by the presence of DBSA in comparison with the bare composite, as shown in Figure 1(b), although the effect of DBSA is not so great because of its lower concentration of DBSA (0.025*M*) in the composite. The increased crystallinity in the presence of DBSA can be explained by the following factors.[37] First, the

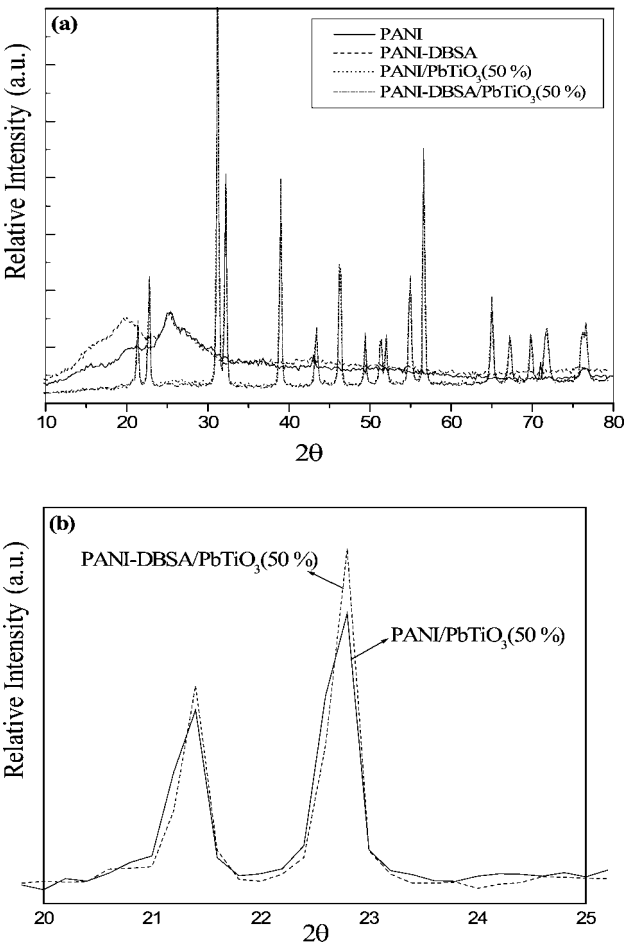

Figure 2 (a) XRD patterns of pure PANI, PANI–DBSA, PANI/$PbTiO_3$ (50%), and PANI–DBSA/$PbTiO_3$ (50%) and (b) an expanded portion comparing the sharpness of the peaks.

alkyl tails of DBSA and the polymer backbones are highly stretched because of the excluded volume effect of the alkyl tails. Second, the microphase-separated nanostructures are self-assembled complex molecules leading to a nonpolar surfactant phase and a polymer phase. The lamellar morphology consisting of alternating polar and nonpolar layers can be predominantly observed at the phases. Third, high degrees of stretching of the polymer chains and the surfactant alkyl tails in mesomorphic phases impart a liquid-crystalline order to the composites.

The easier formation of a micellar structure by DBSA and the role of a surfactant nature can stabilize the dispersion of the PANI–DBSA particles. The hydrophobic tails of free and bonded DBSA molecules are arranged in such a way that they all turn to one another, whereas the hydrophilic groups of the free DBSA turn to the aqueous phase, as shown in Figure 1. The interaction of particles generates an aggregation that further clusters into agglomerates having a size of 50 nm and is located within gel-like units. The formation of these structures is due to the

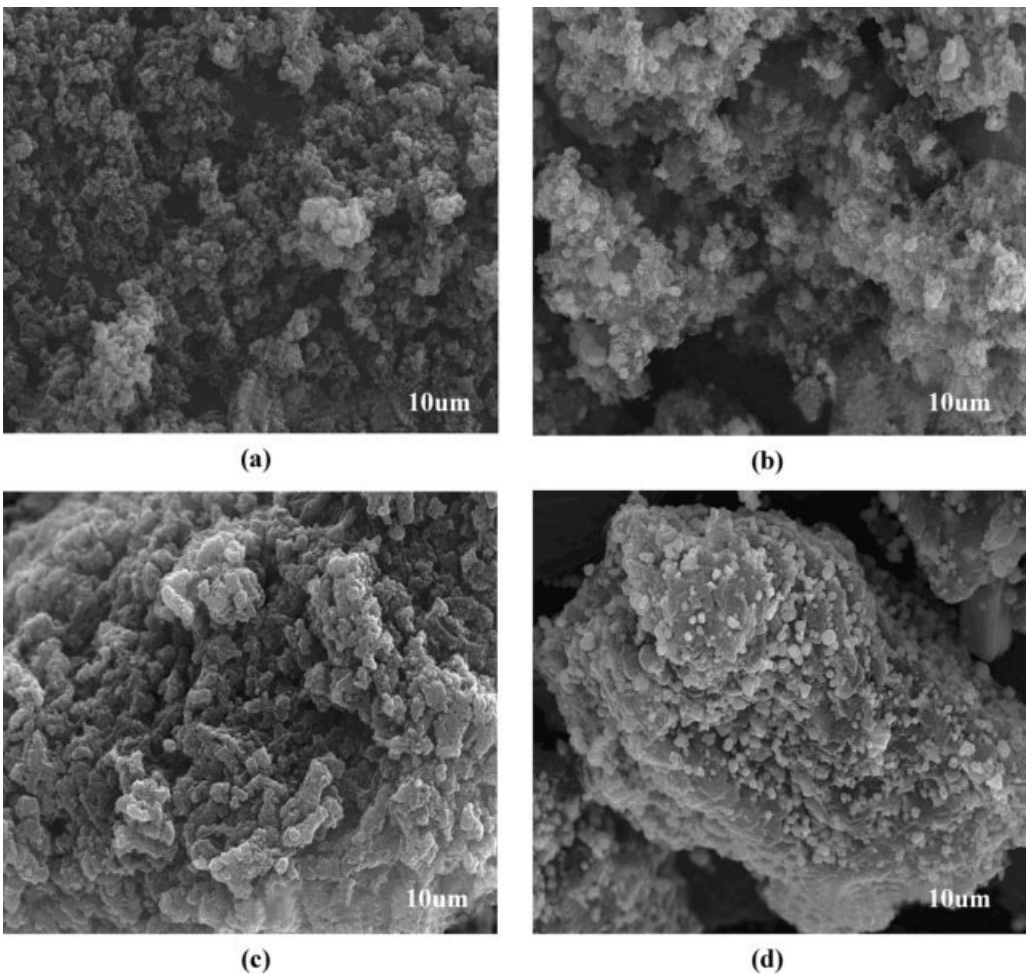

Figure 3 SEM pictures of the surfaces of (a) pure PANI, (b) PANI/$PbTiO_3$ (50%), (c) PANI–DBSA, and (d) PANI–DBSA/$PbTiO_3$ (50%).

hydrogen bonds present between free DBSA molecules. These hydrogen bonds form an infinite network that stabilizes the PANI–DBSA dispersion.[32] These features cause PANI–DBSA/$PbTiO_3$ composites to be more crystalline than PANI/$PbTiO_3$.

Comparison of the surface properties of the polymer composites

Figure 3 shows the scanning electron micrographs of pure PANI, PANI/$PbTiO_3$ (50%), PANI–DBSA, and PANI–DBSA/$PbTiO_3$ (50%). Pure PANI shows an aggregated structure,[17] whereas the PANI/$PbTiO_3$ (50%) composite exhibits an aggregated granular morphology, as shown in Figure 3(b). We obtained an average grain size of about 0.6 μm for PANI/$PbTiO_3$ (10%). The size of the grains increases with the contents of $PbTiO_3$. With an increase in the content of $PbTiO_3$, the composite particles aggregate into a larger size and are visible as a granular shape, which suggests an intermixing of $PbTiO_3$ particles with the PANI matrix.[22] This means that the PANI deposited on the surface of the $PbTiO_3$ particles has an effect on the crystallization performance of PANI/$PbTiO_3$.[37] It shows that the composites have a more ordered arrangement at a higher concentration of oxide (50 wt %) than in the pure PANI.

DBSA forms a micellar structure that acts as a surfactant which stabilizes the dispersion of polymer particles because of the formation of hydrogen bonds between free DBSA molecules, as shown in Figure 3(c).[31,38] These hydrogen bonds form an infinite network that stabilizes the PANI–DBSA dispersion as it forms rodlike structures over the surface in the form of a complex. As a result, the distribution of $PbTiO_3$ in PANI–DBSA/$PbTiO_3$ makes the composite more crystalline than PANI/$PbTiO_3$, as shown in Figure 3(d). As the content of $PbTiO_3$ increases, the particle size also increases. The average grain size is about 0.75 μm for PANI/$PbTiO_3$ (10%). The size of these grains increases with the contents of $PbTiO_3$. This suggests an important result for the incorporation of DBSA into the composite matrix using metal oxide particles related to the crystallin-

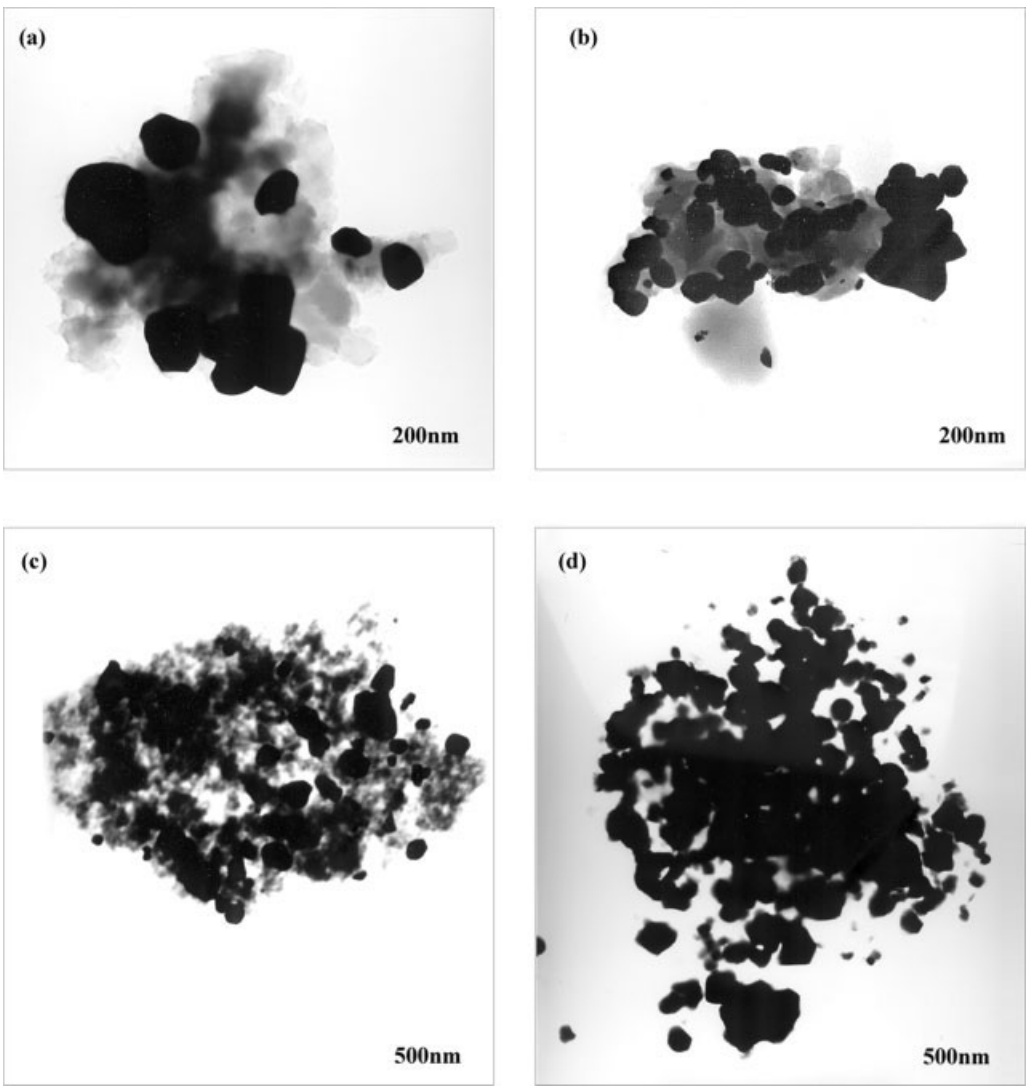

Figure 4 TEM images at different magnifications: (a) PANI/$PbTiO_3$ (50%) and (b) PANI–DBSA/$PbTiO_3$ (50%) at 200 nm and (c) PANI/$PbTiO_3$ (50%) and (d) PANI–DBSA/$PbTiO_3$ (50%) at 500 nm.

ity, as shown in the XRD patterns exhibited in Figure 2. This fact is supported further by the results of TEM discussed later.

The enhanced morphology of the composites of dispersed $PbTiO_3$ particles in the PANI–DBSA matrix was further confirmed by TEM, as illustrated in Figures 4(a–d). The figures show micrographs of PANI/$PbTiO_3$ (50%) and PANI–DBSA/$PbTiO_3$ (50%) with different magnifications of 200 and 500 nm, respectively. It is difficult to distinguish $PbTiO_3$ particles from the polymer matrix when we compare the 500-nm images of PANI–DBSA/$PbTiO_3$ (50%) as shown in Figure 4(c,d). However, a closer look at the same images at 200 nm allows us to identify the free and bound polymer matrix, as shown in Figure 4(a,b). These points confirm that $PbTiO_3$ is better encapsulated/clustered by PANI–DBSA particles than PANI.

Comparison of the thermal behavior for the composites

The TGA thermograms for pure PANI, PANI/$PbTiO_3$ (30%), PANI/$PbTiO_3$ (50%), PANI–DBSA, PANI–DBSA/$PbTiO_3$ (30%), and PANI–DBSA/$PbTiO_3$ (50%) are shown in Figure 5. The composites undergo a three-stage decomposition pattern. The first stage is weight loss, starting from room temperature to 110°C, which corresponds to a loss of water molecules/moisture present in the polymer. The second stage loss, from 110 to 350°C, is associated with a loss of dopant ions[38] from the polymer matrix. This may be assigned to the decomposition of an organic substance present in the composite, which is called the critical temperature. The increase in the critical temperature in PANI–DBSA can be ascribed to the complete decomposition of DBSA, which shows the formation of the PANI–DBSA complex.[39]

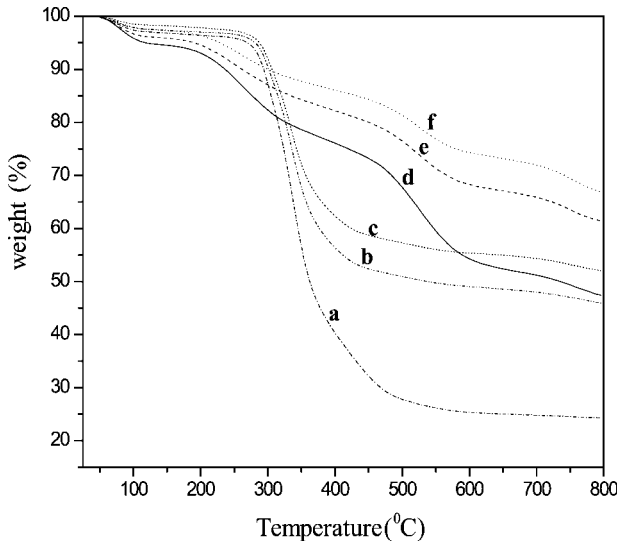

Figure 5 TGA thermograms for (a) PANI–DBSA, (b) PANI–DBSA/$PbTiO_3$ (30%), (c) PANI–DBSA/$PbTiO_3$ (50%), (d) pure PANI, (e) PANI/$PbTiO_3$ (30%), and (f) PANI/$PbTiO_3$(50%).

The third stage of degradation is different between PANI and PANI–DBSA; PANI is in the range of 350–620°C, whereas PANI–DBSA is in the range of 280–500°C. This implies a complete decomposition of the organic polymer.[40] However, the $PbTiO_3$ composite has a little weight loss in the scanned region.[41] The degradation of the polymer occurs slowly between 280 and 500°C and gets faster above 500°C. Figure 5 shows that all $PbTiO_3$ composites have higher decomposition temperatures than pure PANI or PANI–DBSA and that an increase in the content of $PbTiO_3$ for both PANI and PANI–DBSA increases the thermal stability of their composites. The reason for the difference in TGA between the composites can be interpreted in light of the vaporization of DBSA and depression of heat resistance from dilution.

As the degree of initial degradation is not proportional to the contents of the dopant and because the decrease of the initial degradation temperature of the composite becomes much smaller or even negligible when the oxide content reaches a certain level, the degree of the initial degradation ceases to increase after this temperature when the content of the same is beyond the threshold level.[42] All the composites show higher decomposition temperatures when compared to either pure PANI or PANI–DBSA. The increase in the concentration of $PbTiO_3$ in both PANI–DBSA and PANI increases the thermal stability of the composites. This fact confirms that $PbTiO_3$ has a positive influence on the thermal stability of the composites. In other words, $PbTiO_3$ inhibits fast degradation of the polymers.[43] The comparison for the degradation behavior of the composites is summarized in Table I.

TABLE I
Comparison of the Degradation Behavior of PANI, PANI–DBSA, and Their Composites with $PbTiO_3$

Composite	Weight loss (wt %)	
	At 300°C	At 400°C
PANI	82	76
PANI/$PbTiO_3$ (30%)	87	82
PANI/$PbTiO_3$ (50%)	89	86
PANI–DBSA	87	40
PANI–DBSA/$PbTiO_3$ (30%)	90	56
PANI–DBSA/$PbTiO_3$ (50%)	92	62

Electric properties of the composites of PANI/$PbTiO_3$ and PANI–DBSA/$PbTiO_3$

Figure 6 shows a comparison of conductivity values of PANI/$PbTiO_3$ composites for different weight percentages of $PbTiO_3$ at 100 Hz in the presence and absence of DBSA. Here, we can see a drastic change in the conductivity values due to the presence of DBSA. The inclusion of $PbTiO_3$ in the composite has a negative effect on the conducting behavior of PANI. However, the presence of DBSA has brought out an increase in the conductivity of the composite, as shown in Figure 6. This can be due to the enhanced chain links in PANI–DBSA, which stabilize the dispersed particles more than in PANI.[40] In addition, the result can be ascribed to a fast segregation process that takes place in the combined PANI–DBSA polymer aqueous dispersions. The stems of segregation by different surface characteristics of the PANI–DBSA particles and the matrix polymer particles of the surfactant may stabilize the PANI/$PbTiO_3$ particles, as shown in Figure 1. The strong

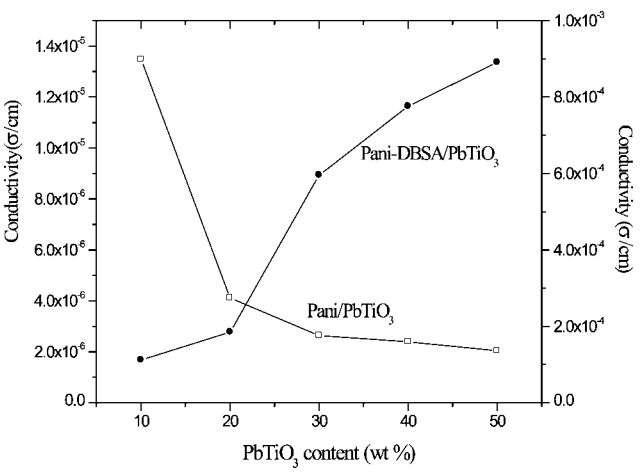

Figure 6 Conductivity of PANI/$PbTiO_3$ and PANI–DBSA/$PbTiO_3$ composites at different weight percentages of $PbTiO_3$ at 100 Hz.

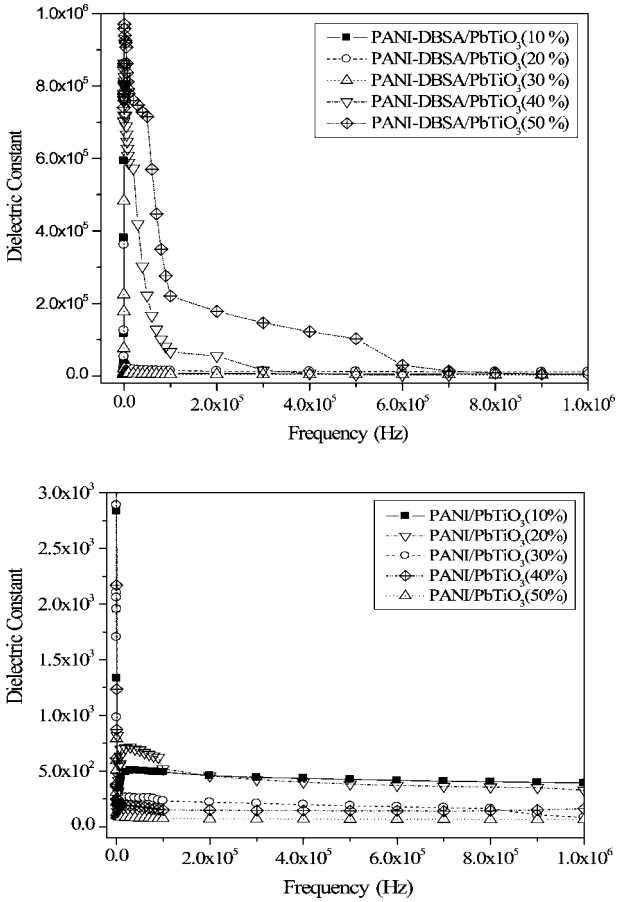

Figure 7 Frequency-dependent dielectric constants of different composites of PANI–DBSA/$PbTiO_3$ and PANI/$PbTiO_3$ at room temperature.

segregation and formation of thin layers of PANI–DBSA yield conductive blends in the composites. The primary PANI particles being generated and aggregated further cluster into agglomerates within gel-like units of DBSA, which is structured because of the formation of hydrogen bonds between free DBSA molecules. The hydrogen bonds help to form an infinite network that can stabilize the PANI–DBSA dispersion more than the PANI dispersion,[32] thereby increasing the conducting properties of the PANI–DBSA/$PbTiO_3$ composite.

The dielectric constant and dielectric loss for the composites of PANI/$PbTiO_3$ and PANI–DBSA/$PbTiO_3$ with different weight percentages of $PbTiO_3$ at an increased frequency are shown in Figures 7 and 8, respectively. The dielectric constant values show a great difference between PANI/$PbTiO_3$ and PANI–DBSA/$PbTiO_3$, as shown in Figure 7. The overall values increase by a magnitude of more than 10^3 in PANI–DBSA/$PbTiO_3$ in comparison with PANI/$PbTiO_3$ with the increase in the $PbTiO_3$ content. However, the values of the dielectric loss do not change significantly in either type. The values decrease with the increase in the $PbTiO_3$ content in the composite even in the presence of DBSA, as shown in Figure 8. The electric behavior of the materials is characterized by the complex dielectric constant or complex permittivity (ε^*):

$$\varepsilon^* = \varepsilon' + j\varepsilon''$$

where ε' is the dielectric constant and ε'' is the dielectric loss.

The dielectric constant and dielectric loss as a function of frequency indicate higher values at lower frequencies and decrease with increasing frequency. Because these composites become more conductive, the permittivity increases because of the space charge buildup at the interfaces between the polymer matrix and $PbTiO_3$ as a result of the difference in the conductivity of the two phases. When we compare the values of the dielectric constant and dielectric loss for both the PANI/$PbTiO_3$ and PANI–DBSA/$PbTiO_3$ composites, PANI/$PbTiO_3$ has smaller dielectric properties than PANI–DBSA/$PbTiO_3$. As we increase the $PbTiO_3$ content in PANI/$PbTiO_3$, its dielectric properties decrease, whereas the dielectric properties increase in the PANI–DBSA/$PbTiO_3$ com-

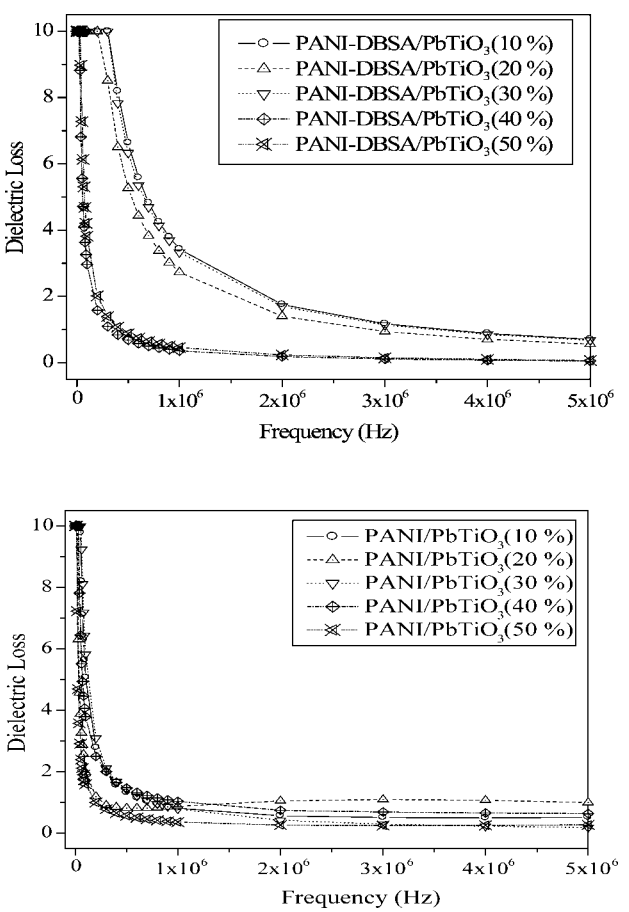

Figure 8 Frequency-dependent dielectric loss of different composites of PANI–DBSA/$PbTiO_3$ and PANI/$PbTiO_3$ at room temperature.

posites. This difference may be ascribed to the fact that PANI/$PbTiO_3$ composites are affected by a decrease in the molecular packing efficiency of their chemical structures with the increasing content of $PbTiO_3$. A low molecular packing order can lead to a decrease in the number of polar groups in the unit of volume. In other words, fewer polarizable groups in a unit of volume may lead to a low dielectric constant.[44,45] The increase in the dielectric properties of PANI–DBSA/$PbTiO_3$ may be attributed to the effect of interfacial polarization, which is known as the Maxwell–Wagner–Sillars effect.[46–48] This is a phenomenon observed in heterogeneous media due to the accumulation of virtual charge at the interfaces of the media.[49] After all, the dielectric properties can be drastically different, depending on the frequency at which the blends are used.

CONCLUSIONS

We have studied the influence of DBSA on the electrical properties of PANI/$PbTiO_3$ composites. Conducting PANI/$PbTiO_3$ composites have been synthesized by the polymerization of aniline with APS as an initiator in both the presence and absence of DBSA. The dispersed $PbTiO_3$ particles remain intact and are preferentially located on the surface where the polymerization of aniline to form PANI occurs in both the presence and absence of DBSA, thus making the polymer more crystalline. The increase in the conducting properties of PANI–DBSA/$PbTiO_3$ reveals the formation of the PANI–DBSA complex structure, which is responsible for the enhancement of such properties.[37] The molecular packing efficiency of PANI/$PbTiO_3$ composites decreases with the increasing content of $PbTiO_3$, which leads to the weakening of the electrical properties. This can be enhanced by the use of DBSA, which increases the packing order by increasing the number of polarizable groups in the polymer matrix. The conductivity of PANI/$PbTiO_3$ is not higher than that of pure PANI and its other composite; the inclusion of DBSA in PANI/$PbTiO_3$ considerably enhances the conductivity of the composites. Furthermore, the other electrical properties, the dielectric constant and dielectric loss, are much affected by the addition of DBSA to the composites. As indicated in previous reports,[10,31,40] DBSA not only acts as a surfactant but also serves as a doping agent to PANI, which increases the charge carriers in the composites and impacts the conductivity and dielectric properties of the composites. This may also be a factor in the increase in conductivity in the composites. It means that a surfactant such as DBSA has an important role in modifying the properties of PANI composites by its incorporation into the composite matrix containing $PbTiO_3$ particles, as it does in the case of PANI with other organic dopants.[44–46] The incorporation of inorganic oxide particles into organic polymers offers the possibility of the formation of a plethora of novel materials with high potential for new applications. For optimal control of the properties of these new materials, it is very important to tailor the formation process from the point of view of the final product.

References

1. Lee, K.; Cho, S.; Park, S. H.; Heeger, A. J.; Lee, C. W.; Lee, S. H. Nature 2006, 441, 65.
2. Macdiarmid, A. G. Synth Met 2002, 125, 11.
3. Nalwa, H. S. Handbook of Advanced Electronic and Photonic Material Devices, Vol. 8; Academic: London, 2000.
4. Cao, Y.; Treacy, G. M.; Smith, P.; Heeger, A. J. Appl Phys Lett 1992, 60, 2711.
5. Lu, J.; Moon, S. K.; Kim, B. K.; Wong, C. P. Polymer 2007, 48, 1510.
6. Novak, P.; Muller, K.; Santhanam, K. S. V.; Hass, O. Chem Rev 1997, 97, 207.
7. Garnier, F.; Horowitz, G.; Ping, X.; Fichou, D. Adv Mater 1990, 2, 592.
8. Li, H. S.; Josowicz, M.; Baer, D. R.; Engelhard, M. H.; Janata, J. J Electrochem Soc 1995, 124, 798.
9. Wang, H. L.; MacDiarmid, A. G.; Wang, Y. Z.; Gebler, D. D.; Epstein, A. J. Synth Met 1996, 78, 33.
10. Rose, T. L.; Antonio, S. D.; Jillson, M. H.; Kron, A. B.; Suresh, R.; Wang, F. Synth Met 1997, 85, 1439.
11. Cao, Y.; Colaneri, N.; Heeger, A. J.; Smith, P. Appl Phys Lett 1994, 65, 2001.
12. Oesterholm, J. E.; Klavetter, F.; Smith, P. Polymer 1994, 35, 131.
13. Okamoto, Y.; Xu, Z. S.; McLin, M. G.; Fontanella, J. J.; Pak, Y. S.; Grenbaum, S. G. Solid State Ionics 1993, 60, 131.
14. Cao, Y.; Qui, J.; Smith, P. Synth Met 1995, 69, 187.
15. Oesterholm, J. E.; Cao, Y.; Klavetter, F.; Smith, P. Polymer 1994, 35, 2902.
16. Yang, C. Y.; Cao, Y.; Smith, P.; Heeger, A. J. Synth Met 1993, 53, 293.
17. de Azevedo, W. M.; de Souza, J. M.; de Melo, J. V. Synth Met 1999, 100, 241.
18. Chwang, C. P.; Liu, C. D.; Huang, S. W.; Chao, D. Y.; Lee, S. N. Synth Met 2004, 142, 275.
19. Ma, Z. H.; Tan, K. L.; Chua, W. S.; Kang, E. T.; Kang, K. G. J Mater Sci: Mater Electron 2000, 11, 311.
20. Ma, Z. H.; Tan, K. L.; Chua, W. S.; Kang, E. T.; Neoh, K. G. Appl Surf Sci 173, 2001, 242.
21. Liu, Y.; O'Keefe, M. J.; Beyaz, A.; Schuman, T. P. Surf Interface Anal 2005, 37, 782.
22. Vishnuvardhan, T. K.; Kulkarni, V. R.; Basavaraja, C.; Raghavendra, S. C. Bull Mater Sci 2006, 29, 77.
23. Basavaraja, C.; Park, D. Y.; Choi, Y. M.; Park, H. T.; Revanasiddapppa, M.; Vishnuvardhan, T. K.; Huh, D. S. Bull Korean Chem Soc 2007, 28, 1.
24. Fusalba, F.; Bélanger, D. J Mater Res 1999, 14, 1805.
25. Yavuz, A. G.; Gok, A. Synth Met 2007, 157, 235.
26. Gok, A.; Omastova, M.; Yavuz, A. G. Synth Met 2007, 157, 23.
27. Gok, A.; Sari, B.; Talu, M. Synth Met 2004, 142, 41.
28. Moulson, A. J.; Herbert, J. M. Electroceramics, 2nd ed.; Wiley: New York, 2003.
29. Xu, Y. Ferroelectric Materials and Their Applications; North-Holland: New York, 1991.

30. Jona, F.; Shirane, G. Ferroelectric Crystals; Dover: New York, 1993.
31. Haba, Y.; Segal, E.; Narkis, M.; Titleman, G. I.; Siegmann, A. Synth Met 2000, 110, 189.
32. Jia, W.; Segal, E.; Kornemandel, D.; Lamhot, Y.; Narkis, M.; Siegmann, A. Synth Met 2002, 128, 115.
33. Wan, M.; Li, M.; Li, J.; Liu, Z. J Appl Polym Sci 1994, 53, 131.
34. Wu, C.-G.; DeGroot, D. C.; Marcy, H. O.; Schindler, J. L.; Kannewurf, C. R.; Liu, Y.-J.; Hipro, W.; Kanatzidis, M. G. Chem Mater 1996, 8, 1992.
35. Kerr, T. A.; Wu, H.; Nazar, L. F. Chem Mater 1996, 8, 2005.
36. Li, X.; Chen, W.; Bian, C.; He, J.; Xu, N.; Xue, G. Appl Surf Sci 2003, 217, 16.
37. Lung Chen, H.; Ni Chang, M. J Polym Res 1999, 6, 231.
38. Patil, S. F.; Bedekar, A. G.; Agashe, C. Mater Lett 1992, 14, 307.
39. Wan, M.; Li, J. J Polym Sci A: Polym Chem 1998, 36, 2799.
40. Kim, S.; Ko, J. M.; Chung, I. J. Polym Adv Technol 1997, 7, 599.
41. Ohara, Y.; Koumoto, K.; Shimizu, T.; Yanagida, H. J Mater Sci 1995, 30, 263.
42. Das, D.; Kar, S.; Chakraborty, S.; Chakraborty, D.; Gangopadhyay, S. J Appl Polym Sci 1998, 69, 841.
43. Somani, P. R.; Marimuthu, R.; Mandale, A. B. Polymer 2001, 42, 2991.
44. Wang, Y. Z.; Hsu, Y. C.; Chou, L. C.; Hsieh, K. H. J Polym Res 2004, 11, 127.
45. Tsotra, P.; Friedrich, K. J Mater Sci 2005, 40, 4415.
46. Deligöz, H.; Yalcinyuva, T.; Özgümüs, S.; Yildirin, S. J Appl Polym Sci 2006, 100, 810.
47. Ku, C. C.; Liepins, R. Electrical Properties of Polymers; Adam Hilger: Bristol, Gimhae City, Kyungnam, South Korea, 1977.
48. Psarras, G. C.; Manolakaki, E.; Tsangaris, G. M. Compos A 2002, 33, 375.
49. Dutta, P.; Biswas, S.; Kumar De, S. Mater Res Bull 2002, 37, 193.